OPTIMAL PAYLOAD TRAJECTORY CHARACTERISTICS FOR WINGED BOOSTER VEHICLES

Jarrell R. Elliott and Timothy R. Rau

NASA Langley Research Center
Langley Station, Hampton, Va.

Presented at the AIAA Guidance, Control, and Flight Dynamics Conference
Atmospheric Flight Mechanics Session,

Huntsville, Alabama
August 14-16, 1967

OPTIMAL PAYLOAD TRAJECTORY CHARACTERISTICS FOR WINGED BOOSTER VEHICLES

Jarrell R. Elliott
Aerospace Engineer
and Timothy R. Rau
Student Trainee
NASA Langley Research Center
Langley Station, Hampton, Virginia

Abstract

The prospective use of space launch vehicles equipped with one or more winged stages to permit recovery and reuse presents an interesting problem in trajectory optimization: Can the lift capability of the vehicle be used to advantage during the atmospheric phase of a boost to orbit trajectory? The results of an analysis in which optimal lifting trajectories of a hypothetical two-stage winged space launch vehicle are compared with nonlifting trajectories for the same vehicle are presented. Fixed geometry wings of various planform areas and weights were added to a basic vehicle of the Saturn V class to arrive at a winged boost-launch system. A horizontal launch take-off mode, which considered the effect of a ground-based acceleration sled, was studied in addition to the conventional vertical launch mode. Increases in weight injected into low altitude orbits of about four percent are possible for vertically launched vehicles using lifting rather than nonlifting trajectories. Ground assisted horizontally launched vehicles can inject about 40 percent more weight into orbit than vertically launched vehicles of the same weight. Increasing first-stage structural weight of the horizontally launched vehicle by one million pounds reduces this figure to 20 percent.

Introduction

An accepted procedure in the design of trajectories for vertical take-off space launch vehicles of today is the use of a maneuver called a gravity turn during atmospheric flight. This gravity-turn maneuver results in a zero angle of attack or nonlifting trajectory. The principal reason for employment of this type of trajectory is the need to keep structural weight to a minimum. Some of the future launch-vehicle concepts being considered, however, are of the recoverable and reusable type which will have considerably different structural requirements. Such vehicle systems may employ rigid wings to provide horizontal landing capability of individual stages. See references 1 to 4 for example. The possibility exists therefore that a favorable advantage may derive from optimal use of the lift capability on the ascent trajectory. In view of this possibility a study was initiated to make a preliminary analysis of optimal lifting trajectories of large winged space launch vehicles propelled by rocket engines.

The object of this study was to determine the changes in the performance capabilities of a selected booster system resulting from optimal use of the lift available from the wing as compared to the zero-lift or gravity-turn performance capability. It was also desired to establish the wing load due to lift during boost resulting from use of optimal lifting trajectories. The trajectory computations were made using a steepest descent computer program which determines the maximum payload trajectory for fixed-propellant weights in each stage. A horizontal take-off (HTO) launch mode is considered in addition to the more conventional vertical take-off launch mode. In the HTO launch mode the effect of a ground acceleration device to accelerate the vehicle to flying speed was considered.

A single basic vehicle consisting of a hypothetical two-stage configuration of the Saturn V class was adopted for use throughout the study. Rigid fixed-geometry wings of various planform areas up to 10,000 square feet were considered attached to the basic vehicle. Additional first-stage structural weight as a result of the wing addition was assumed to vary in direct proportion to the exposed wing planform area. Three different constants of proportionality were used.

Study Assumptions and Procedure

Earth and Vehicle Modeling

The basic configuration consists of a two-stage vehicle of the general class of a Saturn V weighing approximately 6 million pounds at take-off with a thrust at launch of 7.5 million pounds and a second-stage thrust level of 1.5 million pounds. This vehicle, which is capable of injecting approximately 400,000 pounds into a 121-nautical-mile circular orbit, had been studied previously in reference 5 to determine optimal first- and second-stage propellant weights for a maximum payload trajectory based on a gravity-turn first stage. These propellant weights, in addition to other of the weight parameters used in reference 5, were used in the present study for both the VTO and the HTO vehicle. The vehicle, engine, and weight data characterizing the basic configuration are given in table I. The structural weight given includes both fixed hardware items and propellant tankage weight. In the study the changes in first-stage structural weight required to accommodate increased airloads, that required for additional fixed hardware items to accomplish recovery, and that due to wing structure were not separately considered. The change in first-stage structural weight was determined by adding additional weight in direct proportion to the exposed area of the wing using constants of proportionality of 0, 10, and 20 pounds per square foot of area.

A 121-nautical-mile circular orbit, also used in reference 5, was taken as the target orbit. The earth model used was a spherical rotating earth with the 1959 ARDC model atmosphere. Launches were assumed to take place from the Eastern Test Range on a launch azimuth of 90°.

Aerodynamics

The external configuration was assumed to be as shown in figure 1 where the vehicle dimensions shown are intended only as a guide to indicating size. The wing is a clipped delta, of aspect ratio 2, with a 50° leading-edge sweep angle and a tip-to-root chord ratio of 0.254. Wings of this same geometry having exposed planform areas of 2500, 5000, 7500, and 10,000 square feet were assumed to

be attached to the cylindrical first stage of the basic vehicle.

The aerodynamic data of the basic vehicle generally conform to that of the Saturn V vehicle. Aerodynamic data for the wings and the wing-body combinations were obtained by standard techniques described in references 6 and 7. The aerodynamic coefficients for the body-alone and each wing-body combination studied are plotted against Mach number in figure 2. All aerodynamic coefficients are based on the cross-sectional area of the first stage resulting in a reference area of 855 square feet. (See table I.) Presented in the figure are profile-drag coefficient of the body alone, incremental profile-drag coefficient of each wing to be added to that of the body alone to obtain the total profile-drag coefficient, and lift-curve-slope coefficient for each configuration. The values shown at the intersection of the straight-line segments in the figure were input points to the computer program which used linear interpolation to obtain intermediate values of the coefficients.

The induced drag coefficient for all configurations was computed from the equation

$$C_{D_i} = K \frac{S_R}{S_{WB}} C_L^2 \qquad (1)$$

where S_R/S_{WB} is the ratio of reference area to total wing area and K is a factor dependent on Mach number. A plot of the factor K against Mach number with a table of values of the ratio S_R/S_{WB} as an inset are shown in figure 3. The K factors in the supersonic range were extracted from data in reference 8. Linear extrapolation was used in going from supersonic to hypersonic and the data were faired from 0.29 at a Mach number of 2.0 to a value of 0.20 at a Mach number of 1.0 and below for the transonic and subsonic Mach number range. In order to convert the data to the desired reference area the ratio of reference area to total wing area is required where total wing area includes that portion of the wing interior to the body. For the zero wing area case a value of 0.3 for this ratio was chosen as being most representative of drag due to the lift for the body alone.

Trajectory Calculations

The trajectory calculations were made using a digital computer program, described in reference 9, which maximizes the weight injected into orbit for the fixed stages of this study. This program is based on the method of steepest descent and the sequence of operations used is such that the final trajectory (optimal in the sense of steepest descent) has only minor deviations from the desired terminal values of the constrained quantities; velocity, altitude, flight-path angle, and propellant used.

A basic set of 13 trajectory cases was established for each type of launch trajectory; the gravity turn VTO, the lifting VTO, and the lifting HTO. These 13 cases were the possible different vehicles resulting from combinations of the five wing areas (S_W); 0, 2500, 5000, 7500, and 10,000 square feet, and the three wing weight factors (K_W); 0, 10, and 20 pounds per square foot. A few miscellaneous cases investigating the effect of various changes in the characteristics of the launch vehicles have also been included. Details of the procedure followed in computing trajectories for the vertical take-off launch and the horizontal take-off launch are given below.

VTO.- The vehicle was assumed to thrust vertically for 17.1 seconds after which the relative velocity vector was rotated instantaneously downward from 90° to 86° for the lifting trajectory cases and for the gravity turn trajectories to the optimal value of the flight-path angle (or, as it is sometimes called, the kick angle) as determined by the program. Early attempts to optimize the kick angle for the lifting trajectories were terminated since the values computed approached those of the HTO cases and were therefore not characteristic of a vertical take-off launch. For the same reason, it was necessary to specify that a gravity turn trajectory be followed for 15 seconds after the vertical take-off phase. Thus each of the lifting trajectories followed a prespecified program for the first 32.1 seconds of flight. Nine cases were computed in addition to the 26 basic cases using modified values of the lift and profile-drag coefficient. A tabulation and summary of all VTO cases is presented in table II.

HTO.- As previously mentioned, a ground acceleration device, a powered sled or catapult, was considered in conjunction with the horizontal launch mode. This device was assumed to accelerate the vehicle to a velocity of 650 feet per second without using any of the internal propellant of the vehicle for all HTO cases except two. (While the method of generating this acceleration and the power source will be left undefined, a possible means is use of the 7.5-million-pound thrust vehicle engine using propellant supplied from tanks in the carriage or sled.) These two cases were computed assuming that some portion of the internal fuel was required to accelerate to 650 fps; one assuming that 6.4 seconds of burn time was required and the other that 16.1 seconds of burn time was required. These times correspond to the time required to accelerate to 650 fps from 400 and 0 fps, respectively, using the thrust acceleration of the vehicle and assuming a massless frictionless carriage or launch sled. Three additional cases showing the variation of injected weight with first-stage structural weight were also computed. In all cases the attitude of the vehicle at take-off was assumed to be the optimal attitude as computed by the optimization program. A tabulation and summary of all HTO cases is given in table III.

Results

In order that comparisons of weight injected into orbit might be made easily and quickly the performance results are presented in terms of percentage increase (or decrease) in injected weight over that of case 1 (a gravity turn VTO launch with the basic (no wing) vehicle). The injected weight for this case was determined to be 392,997 pounds. Thus 1 percent represents about 4000 pounds of injected weight. It should be noted that throughout this report the results are in terms of injected weight rather than payload weight since the structural weight of the second stage would probably be different for each of the different trajectories studied.

In addition to the performance results, a few remarks about the overall trajectory characteristics will be made as well as a brief discussion of the wing load due to lift during boost and wing loading during stage-one recovery.

Vertical Take-Off

Performance results.- The results of the study of the VTO launch mode are summarized in figure 4 and table II. Figure 4(a) and figure 4(b) present the percentage change in injected weight plotted against wing area for the basic set of 13 cases for the gravity-turn and lifting trajectories, respectively.

A linear variation of injected weight with wing area for each of the wing weight factors is shown in figure 4(a) for the ballistic or gravity turn trajectories. The data points have been faired with straight lines with the only significant deviation being the 10,000-square-foot 20-psf data point. The regularity of these data lends some confidence to the results and to the steepest descent program being used since each data point represents a final optimal trajectory which was obtained only after several iterations. Although the curves for wing weight factors of 10 and 20 psf are influenced by structural weight changes, the variation in injected weight for K_W equal to zero is due entirely to additional profile drag due to the presence of the wing. The increment between curves for constant values of K_W is due to first-stage structural weight changes. It may be seen that the performance loss due to wing profile drag is equal to the performance loss due to a wing weight factor of about 2.3 psf.

Weight injected into orbit through optimal use of the lift capability is summarized in figure 4(b). In addition to the 13 basic cases some additional data points computed in an attempt to separately evaluate optimal thrust attitude pointing effects and optimal lift effects, both of which play an important part in accomplishing performance gains over the comparable gravity-turn trajectories, are shown. These data points are indicated with flags as noted on figure 4(b) and were obtained by setting the lift coefficient to zero.

Use of the lift capability of the winged vehicles shows a 2- to 4-percent performance gain in injected weight over winged vehicles using a gravity-turn trajectory, which is an increase of 8 to 16 thousand pounds of injected weight. Thus if a vehicle is equipped with a wing to permit recovery, the lift available during ascent may be used in an optimal fashion to at least partially offset launch trajectory performance degradation due to the combined effects of increased drag and weight. The performance gain of about 4 percent, which occurs at large values of wing area, probably represents the maximum possible performance gain from lift since the slopes of the lifting trajectory curves and the gravity-turn trajectory curves (for constant K_W) are the same, or nearly so, at the larger values of wing area. This is an indication that little or no additional gain may be derived from lift for wings larger than 10,000 square feet.

The three flagged data points on figure 4(b), as previously mentioned, were used to separately estimate the effect of optimal pointing and optimal lift. Referring back to figure 4(a), a 2.5-percent decrease in performance for a 10-psf, 5000-square-foot wing may be noted for the gravity-turn ascent. The same wing with no lift but using optimal pointing (the flagged symbol at S_W = 5000 sq ft in figure 4(b)) shows only a 1-percent decrease. Optimal use of the lift shows a 0.7-percent increase. This results in an overall performance gain of 3.2 percent by use of a lifting trajectory of which about half is due to lift and the other half is due to optimal thrust pointing. For the 0- and 10,000-square-foot wing area cases, the data show a performance gain of about 1.0 and 1.3 percent, respectively, from optimal thrust pointing alone over the gravity turn. These three data points indicate that of the gains shown by the lifting trajectories over the gravity-turn trajectories, some $1\frac{1}{2}$ percent, or 6000 pounds, may be attributed to optimal thrust pointing. In the case of the basic vehicle use of the lift results in about the same injected weight as optimal pointing without lift.

Figure 5 presents the results of a brief investigation of the influence of profile-drag variations on performance. The figure shows a linear variation of injected weight increase with decrease in profile-drag coefficients. The slopes are -0.0335 and -0.0458 (percent increase in weight injected per percent decrease in profile-drag coefficient) for the basic vehicle and 5000-square-foot wing vehicle, respectively. The results for the zero wing case shown here would also apply to the gravity-turn case. This shows that about 1400 additional pounds of injected weight, most of which could presumably be payload, could be injected into orbit by an overall 10-percent decrease in the profile-drag coefficient.

Two runs varying profile drag were computed to evaluate the performance degradation due to the high initial value of drag coefficient in the 0 to 0.15 Mach number range which results from the base pumping action of the rocket engines. A constant value of profile-drag coefficient of 0.44 for the basic vehicle was used in each case, one a zero wing case and the other a 5000-square-foot wing case. This variation in the drag coefficient resulted in less than 0.05-percent change in injected weight. These results are shown in table II.

Trajectory characteristics.- A representative set of cases, listed in table IV, have been chosen to illustrate the general characteristics noted in the trajectory data. Where it was considered informative and necessary to indicate trends in the data, portions of the time histories of other cases, as noted in figure 6, have been included. Time histories of altitude, dynamic pressure, lift force, and angle of attack during atmospheric flight are shown in figure 6. The time history of thrust attitude with respect to the local horizontal is shown in figure 7.

The first-stage time histories show that the use of a lifting trajectory rather than a gravity-turn trajectory results in lower flight altitude and higher flight dynamic pressure. As wing area increases, the lift increases, flight altitude is lowered, angle of attack is reduced, and maximum dynamic pressure increases. Maximum lift occurs prior to maximum dynamic pressure. The highest value of maximum dynamic pressure of the lifting

cases is more than twice that of a gravity-turn trajectory.

Only minor differences are evident in the thrust-attitude time histories after stage 1. However, during first-stage flight significant increases in pitch-attitude rate may be noted with increases in wing area. The vehicles with wings pitch over rapidly, overshooting 40° pitch attitude which appears to be the desired steady-state value, and return with positive pitch-rate values to a pitch attitude near 40° during stage 1 flight. A nearly linear pitch rate characterizes the remainder of the flight.

The wing load due to lift for both the VTO vehicle and the HTO vehicle will be discussed after the presentation of HTO results.

Horizontal Take-Off

Performance results.- The results of the HTO launch study are summarized in figures 8, 9, and 10. A tabular summary of the HTO results is also given in table III.

The percentage increase in injected weight over that of case 1 is plotted against wing area for the basic set of 13 cases in figure 8. From the data, it may be seen that the weight injected into orbit is essentially independent of wing area. This is most readily seen for the zero wing weight factor cases. There does exist, however, a linear variation of injected weight with first-stage structural weight over the weight range shown. The injected weight of horizontally launched vehicles is about 40 percent higher than that of vertically launched vehicles of the same structural weight. Some of this increase is due to the assumption that the ground acceleration device accelerates the vehicle to a take-off velocity of 650 feet per second using no internal vehicle propellant. For a particular case (a 10-psf, 5000-sq-ft wing), the effect of using some portion of the internal propellant in accelerating to take-off velocity is shown in figure 9. The time that the engine is on before reaching the take-off velocity is shown as the abscissa on this figure and the ordinate is the percent change in injected weight. The data points at 6.4 and 16.1 seconds represent the time required to accelerate the vehicle to 650 fps from 400 and 0 fps, respectively, assuming a massless, frictionless vehicle support system. The loss in injected weight is about 2100 pounds or one-half of 1 percent for each second of engine-on time. Even though system performance is computed in this manner, appreciable increases in injected weight using HTO rather than VTO are still possible under the assumptions used. However, more consideration should be given to the variation of injected weight with structural weight changes using a somewhat different approach than used in the data of figures 8 and 9. Shown in figure 10 is injected weight plotted against first-stage structural weight for a 5000-square-foot wing case assuming zero engine-on time before reaching take-off velocity. This figure enables a more realistic evaluation of the performance capability to be made since for a HTO launch both first- and second-stage structural weight would increase over the values shown in table I. The data show that the gain in injected weight due to horizontal launching is reduced from 42 percent to 32 percent by doubling the structural weight of the basic vehicle. Even with a sixfold increase in structural weight as compared to the basic vehicle, a gain in injected weight of 10 percent is obtained.

Trajectory characteristics.- First-stage time histories of altitude, dynamic pressure, lift, and angle of attack are presented in figure 11 for wing areas of 0, 5000, and 10,000 square feet with a wing weight factor of 10 pounds per square foot. The altitude time histories show that the HTO vehicle tends to fly at a higher altitude than the VTO vehicle. It differs from the VTO in that as wing area increases the flight altitude increases, whereas in the VTO case the flight altitude decreased with increasing wing area.

Maximum dynamic pressure occurs earlier in flight for the HTO vehicle than the VTO vehicle and has a trend again opposite to that of the VTO case, that is, maximum dynamic pressure decreases with increases in wing area. Maximum dynamic pressure for the 10,000-square-foot wing for both the VTO and the HTO cases are about the same value.

Lift varies from a large positive value at or near take-off to a large negative value at around 40 to 50 seconds of flight time. Both the positive and negative magnitudes increase as wing area increases. The ratio of maximum positive lift to maximum negative lift is about 2 and is independent of wing area. The characteristics of the angle-of-attack time histories are similar for all the wing areas.

The dashed curve shown on the thrust-attitude time histories of figure 12 was used as the guessed thrust-attitude time history for all HTO cases so as to remove the influence of different guessed thrust-attitude time histories. The thrust-attitude time histories are very nearly the same after stage 1 separation. However, the HTO cases differ from the VTO cases in that the thrust attitude is negative for almost all of stage 2 whereas for the VTO case the thrust attitude was positive except during the last few seconds of flight. Pitch-attitude rate is initially positive but becomes negative after about 20 seconds and remains negative thereafter. The largest values of thrust attitude occur for the largest wing area. Maximum pitch-attitude rate was less than three degrees per second.

Wing load due to lift.- Maximum values of the ratio of lift force to total wing area (hereafter called lift-load ratio) during boost for both the VTO and HTO cases are shown plotted against exposed wing area in figure 13.

The lift used represents an average value over about 5 seconds of flight during the time of maximum lift. The lift-load ratio for both types of launch decreases nonlinearly with wing area varying from 600 to 300 psf for the VTO vehicle and from 900 to 500 psf for the HTO vehicle. The HTO vehicle lift-load ratio is roughly 50 percent higher than VTO vehicles of the same wing area. The ratio of vehicle weight to total wing area, wing load factor, during stage 1 recovery is shown at the bottom of figure 13 for a wing weight factor of 20 psf. The lift-load ratio is larger by a factor of six or more than this wing load factor indicating that lift-load ratio would dictate the wing structural design.

Conclusions

For winged vertically launched vehicles a lifting trajectory may be used to increase performance, in terms of weight injected into low-altitude orbits, 3 to 4 percent over nonlifting trajectories. However, some of this increase, about $1\frac{1}{2}$ percent, is due to optimization of thrust vector attitude, not the lift of the vehicle. The lifting trajectories are characterized by lower flight altitudes and higher dynamic pressures than the nonlifting trajectories. Flight altitude decreases and dynamic pressure increases with increasing wing area.

The use of a ground assisted horizontal launch rather than a vertical launch results in performance gains of about 40 percent for a vehicle with the same structural characteristics. This percentage is reduced by about 5 percent for each 10 seconds of engine-on time before take-off. First-stage structural weight increases further reduce this percentage; by 22 percent for one million additional pounds above the basic vehicle structural weight, and by 34 percent for two million additional pounds.

The trajectories of horizontally launched vehicles are higher in both altitude and dynamic pressure than vertically launched vehicles. Decreases in dynamic pressure and increases in altitude occur with increases in wing area. Vehicle pitch-attitude rate is positive for approximately the first 20 seconds of flight after which it becomes and remains negative.

The wing load due to lift of horizontally launched vehicles is about 50 percent higher than that of vertically launched vehicles. The wing load due to lift during ascent is larger by a factor of six or more than the wing loading during recovery of the first stage.

References

1. Reusable Launch Systems. Aeronautics and Astronautics, Vol. II, No. 1, Jan. 1964.

2. Vaglio-Laurin, Roberto; and Fink, Reinald G.: Reusable Space Launch Vehicle Concepts: Outlook 1965. SAE Paper No. 650801, presented at National Aeronautic and Space Engineering and Manufacturing Meeting, Oct. 1965.

3. Speith, C. W.: The Economic Justification of Reusable Rocket Vehicles. SAE Paper No. 650802, presented at National Aeronautic and Space Engineering and Manufacturing Meeting, Oct. 1965.

4. Kelber, Charles C.: Future Space Launch Vehicles: Expendable or Recoverable? Paper presented at the Sixth International Symposium on Space Technology and Science, Tokyo, Japan, Dec. 1965.

5. Teren, Fred; and Spurlock, Omer F.: Payload Optimization of Multistage Launch Vehicles. NASA TN D-3191, 1966.

6. Douglas Aircraft Co., Inc.: USAF Stability and Control Handbook. U.S. Air Force, Oct. 1960.

7. Pitts, William C.; Neilsen, Jack N.; and Kaattari, George E.: Lift and Center of Pressure of Wing-Body-Tail Combinations at Subsonic, Transonic, and Supersonic Speeds. NACA Rept. 1307, 1957.

8. Brockway, Daniel J.: A Rapid Method of Determining the Drag Due to Lift of Wing-Body Combinations at Supersonic Speeds. Bureau of Aeronautics Rept. No. DR-1851, 1957.

9. Willwerth, Robert E., Jr.; Rosenbaum, Richard C.; and Chuck, Wong: PRESTO - Program for Rapid Earth-To-Space Trajectory Optimization. NASA CR-158, 1965.

TABLE I.- VEHICLE, ENGINE, AND WEIGHT DATA

	Stage	
	First	Second
Thrust (vac), lb	7.5×10^6	1.5×10^6
Specific impulse (vac), sec	305	428
Propellant weight, lb	3.98×10^6	1.276×10^6
Structural weight, lb	364.4×10^3	112.1×10^3
Nozzle exit area, sq ft	550.4	----------
Aerodynamic reference area, sq ft	855	----------
Coast period at stage burnout, sec	3.3	

TABLE II.- TABULATION AND RESULTS SUMMARY - VERTICAL TAKE-OFF

Case no.	Wing area, 1000 sq ft	Wing weight factor, lb/sq ft	Injected weight, lb	Percent increase in injected weight over case 1	Take-off weight, lb	Initial flight-path angle for gravity-turn trajectories, deg
1	0	--	392,997	0	6,013,387	89.17
2	2.5	0	391,883	-.28	6,012,279	89.17
3	2.5	10	388,040	-1.26	6,033,439	89.23
4	2.5	20	384,267	-2.22	6,054,655	89.28
5	5.0	0	390,868	-.54	6,011,266	89.17
6	5.0	10	383,275	-2.47	6,053,675	89.28
7	5.0	20	375,842	-4.36	6,096,241	89.38
8	7.5	0	389,981	-.77	6,010,378	89.18
9	7.5	10	378,739	-3.63	6,074,141	89.33
10	7.5	20	367,937	-6.38	6,138,322	89.47
11	10.0	0	389,113	-.99	6,009,509	89.19
12	10.0	10	374,188	-4.79	6,094,587	89.38
13	10.0	20	360,319	-8.32	6,180,703	89.54
14	0	--	399,907	+1.76	6,020,368	
15	2.5	0	402,658	+2.46	6,023,028	
16	2.5	10	399,066	+1.54	6,044,437	
17	2.5	20	395,529	+.64	6,065,892	
18	5.0	0	402,854	+2.51	6,023,188	
19	5.0	10	395,836	+.72	6,066,159	
20	5.0	20	389,089	-.99	6,109,411	
21	7.5	0	401,984	+2.29	6,022,409	
22	7.5	10	391,666	-.34	6,087,073	
23	7.5	20	381,944	-2.81	6,152,351	
24	10.0	0	400,891	+2.01	6,021,297	
25	10.0	10	387,457	-1.41	6,107,815	
26	10.0	20	373,004	-5.08	6,193,288	
27	0	--	400,251	+1.85	6,021,009	Lift = 0
28	5.00	10	389,103	-.99	6,059,858	Lift = 0
29	10.00	10	379,469	-3.44	6,099,860	Lift = 0
30	0	--	401,227	+2.10	6,021,669	90% C_{D_o} (S_W = 0)
31	0	--	403,260	+2.61	6,023,684	75% C_{D_o} (S_W = 0)
32	0	--	400,177	+1.81	6,020,576	C_{D_o} = Constant MN $\leq$ 0.6
33	5.0	10	397,642	+1.18	6,067,977	90% C_{D_o} (S_W = 5000)
34	5.0	10	400,389	+1.88	6,070,766	75% C_{D_o} (S_W = 5000)
35	5.0	10	395,986	+.76	6,066,329	C_{D_o} = Constant MN $\leq$ 0.6

TABLE III.- TABULATION AND RESULTS SUMMARY - HORIZONTAL TAKE-OFF

Case no.	Wing area, 1000 sq ft	Wing weight factor, lb/sq ft	Injected weight, lb	Percent increase in injected weight over case 1	Weight at engine ignition, lb	First-stage structural weight, 1000 lb
H 1	0	--	560,050	42.51	6,180,448	364.4
H 2	2.5	0	559,717	42.42	6,180,111	364.4
H 3	2.5	10	556,875	41.70	6,202,270	389.4
H 4	2.5	20	554,099	40.99	6,224,496	414.4
H 5	5.0	0	560,621	42.65	6,181,019	364.4
H 6	5.0	10	555,043	41.23	6,225,437	414.4
H 7	5.0	20	549,599	39.85	6,269,994	464.4
H 8	7.5	0	560,662	42.66	6,181,060	364.4
H 9	7.5	10	552,358	40.55	6,247,756	439.4
H 10	7.5	20	544,365	38.52	6,314,763	514.4
H 11	10.0	0	560,653	42.66	6,181,050	364.4
H 12	10.0	10	549,661	39.86	6,270,056	464.4
H 13	10.0	20	539,293	37.23	6,359,688	564.4
*H 14	5.0	10	520,811	32.52	6,191,209	414.4
**H 15	5.0	10	541,556	37.80	6,217,955	414.4
H 16	5.0	--	523,466	33.18	6,508,265	728.8
H 17	5.0	--	469,049	19.35	7,182,643	1,457.6
H 18	5.0	--	431,570	9.81	7,873,967	2,186.4

*$V_{ignition}$ = 0.

**$V_{ignition}$ = 400 fps.

TABLE IV.- REPRESENTATIVE CASES FOR TRAJECTORY CHARACTERISTICS STUDY

Case no.	S_W, sq ft	K_W, psf	Type of trajectory
1	0	--	Gravity turn
14	0	--	Lifting
19	5,000	10	Lifting
25	10,000	10	Lifting

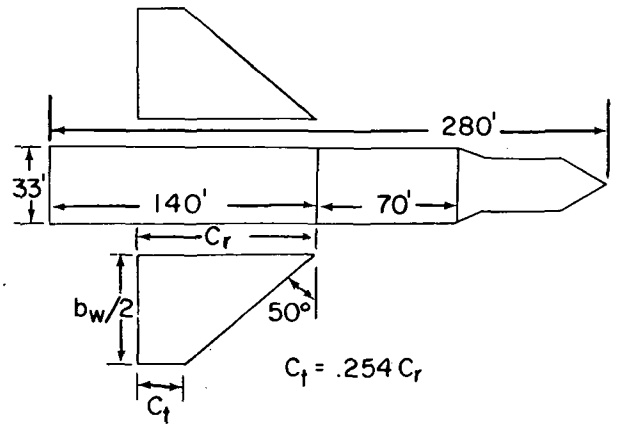

Figure 1.- Vehicle external configuration.

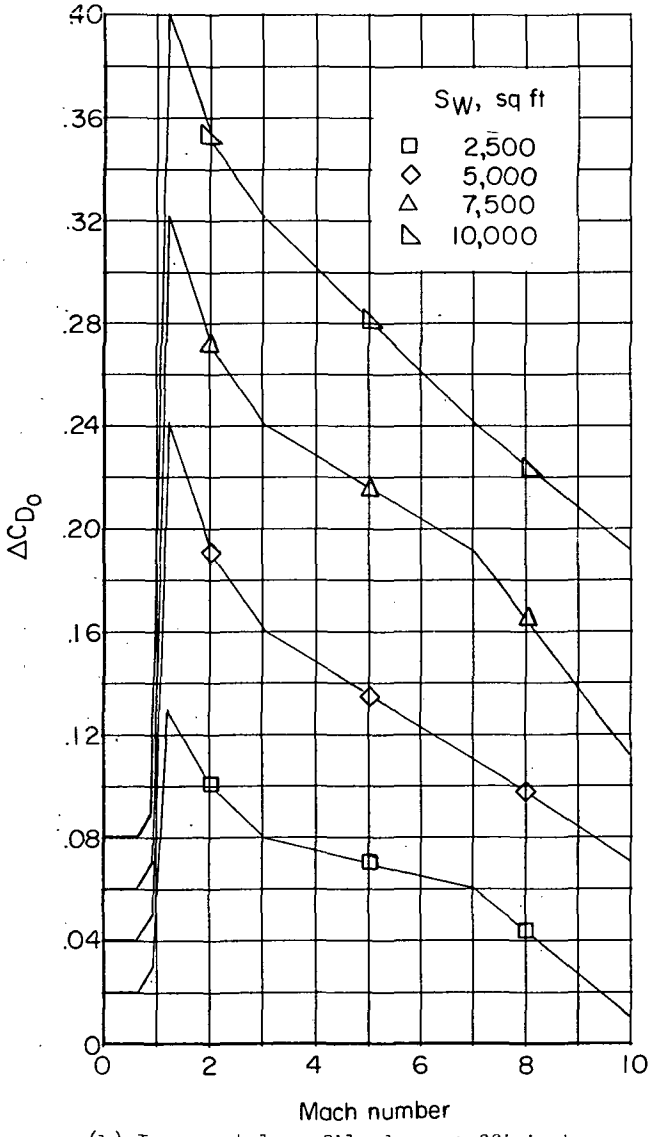

(b) Incremental profile drag coefficient due to wing.

Figure 2.- Continued.

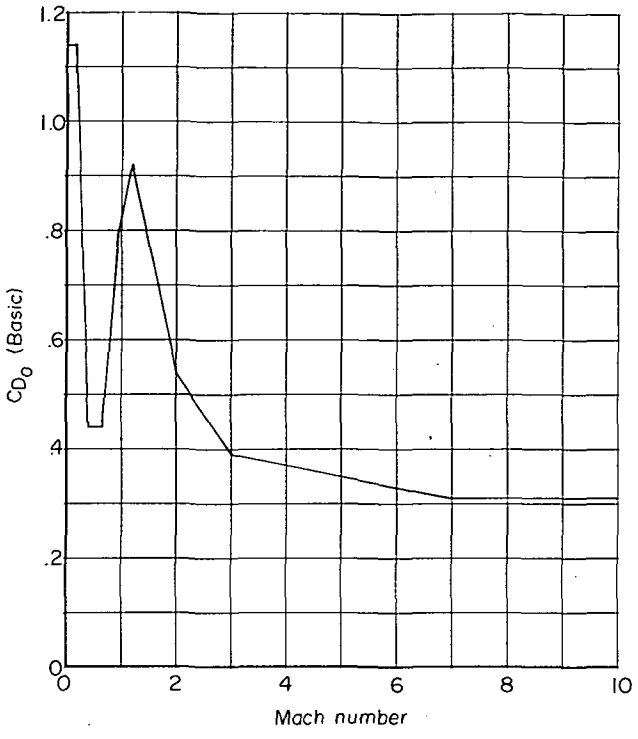

(a) Profile drag coefficient, basic (no wing) vehicle.

Figure 2.- Aerodynamic coefficients plotted against Mach number.

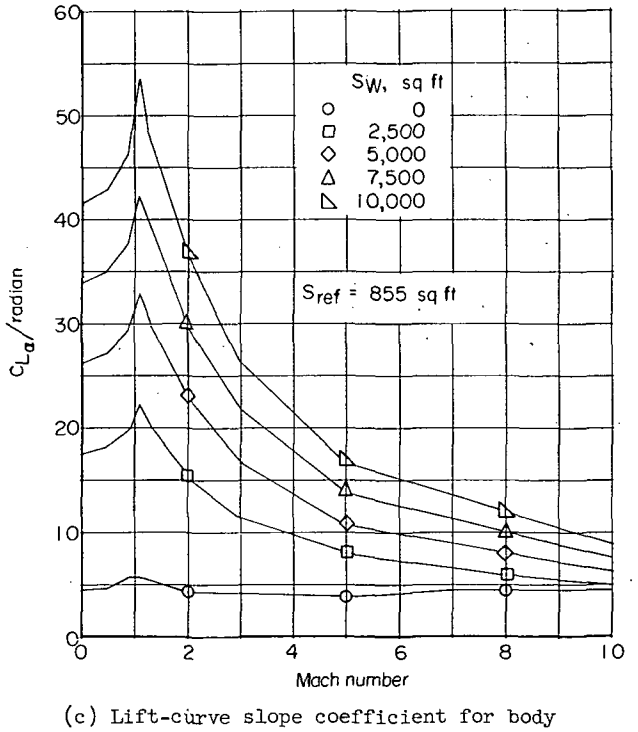

(c) Lift-curve slope coefficient for body and body plus wing.

Figure 2.- Concluded.

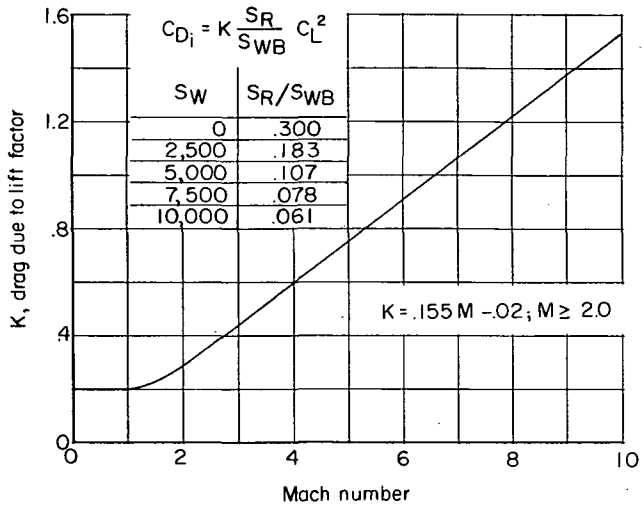

Figure 3.- Variation of factor used in computing induced drag coefficient with Mach number.

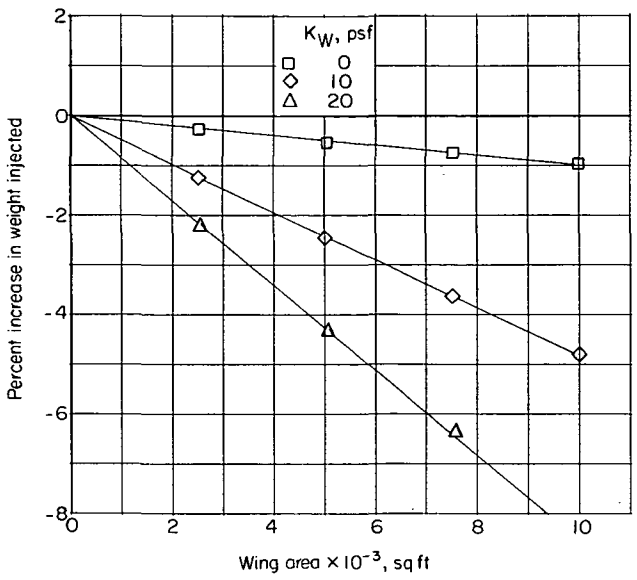

(a) Gravity turn trajectory.

Figure 4.- Variation of percentage increase in injected weight with wing area for wing weight factors of 0, 10, and 20 psf. VTO.

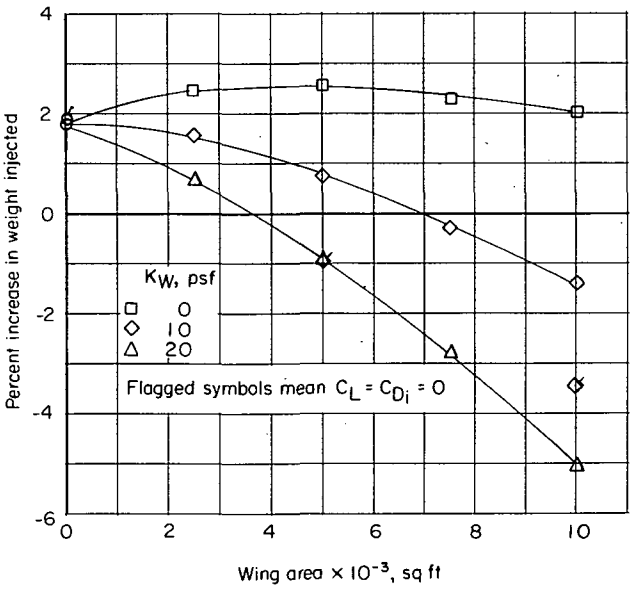

(b) Lifting trajectory.

Figure 4.- Concluded.

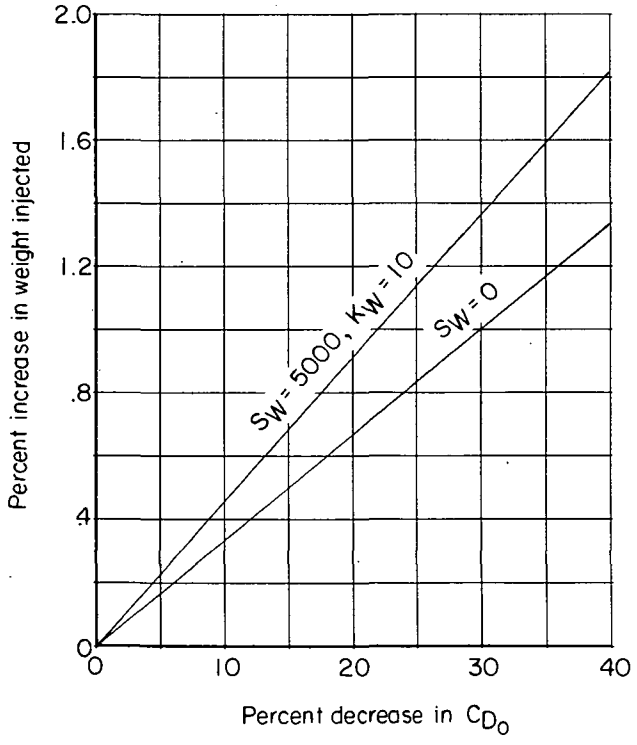

Figure 5.- Effect of reduced profile drag coefficient on injected weight.

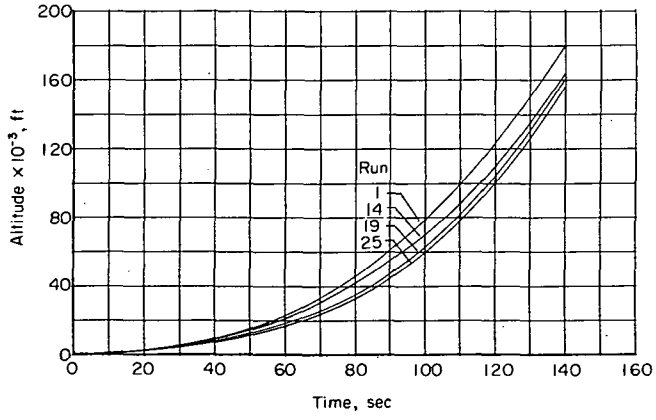

(a) Altitude.

Figure 6.- Time histories of representative cases during atmospheric flight. VTO.

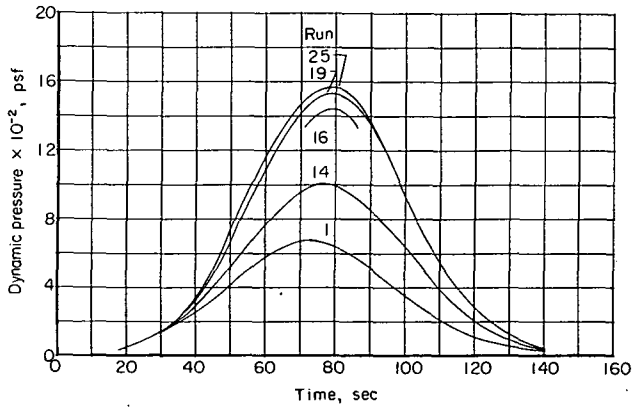

(b) Dynamic pressure.

Figure 6.- Continued.

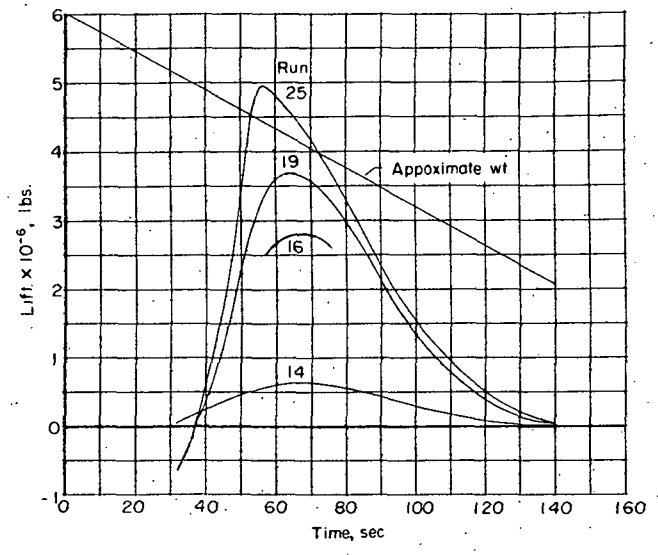

(c) Lift.

Figure 6.- Continued.

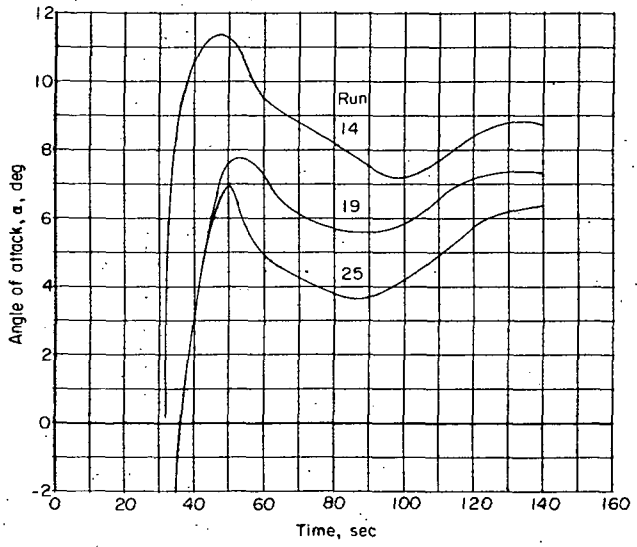

(d) Angle of attack.

Figure 6.- Concluded.

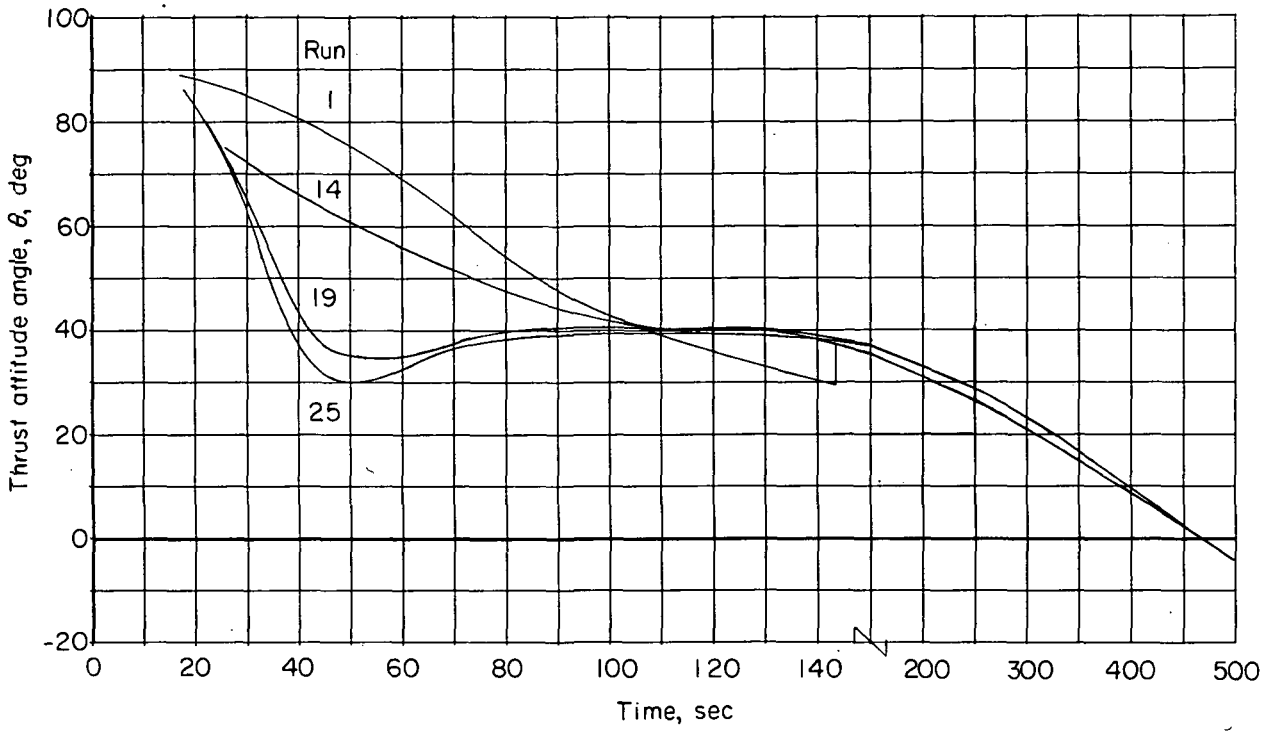

Figure 7.- Vehicle thrust attitude time history. VTO.

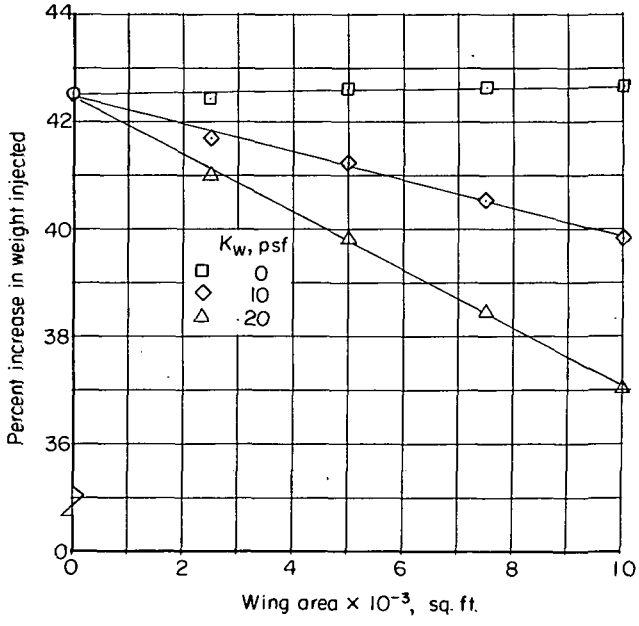

Figure 8.- Variation of percentage increase in injected weight with wing area wing weight factors of 0, 10, and 20 psf. HTO.

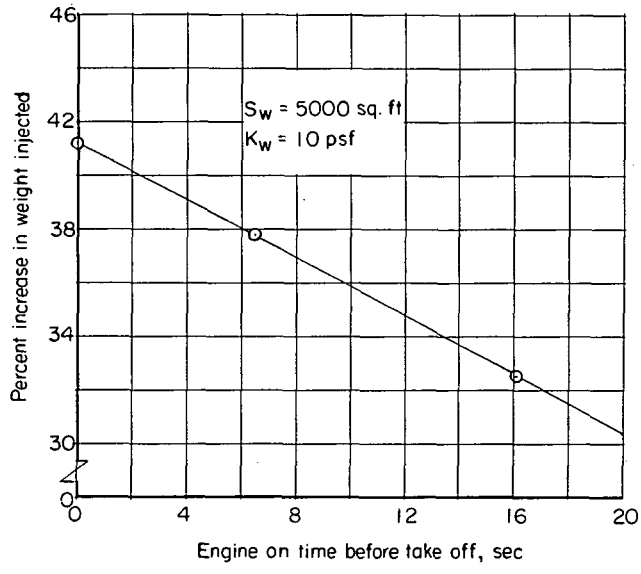

Figure 9.- Variation of percentage increase in injected weight with engine on time before take-off. HTO.

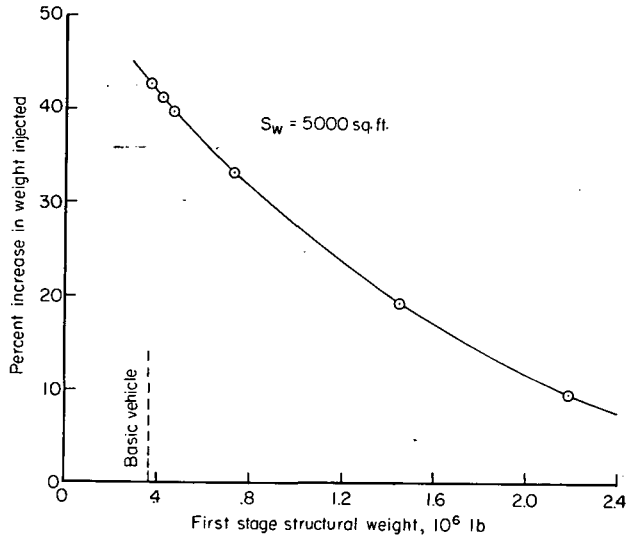

Figure 10.- Variation of percentage increase in injected weight with first stage structural weight.

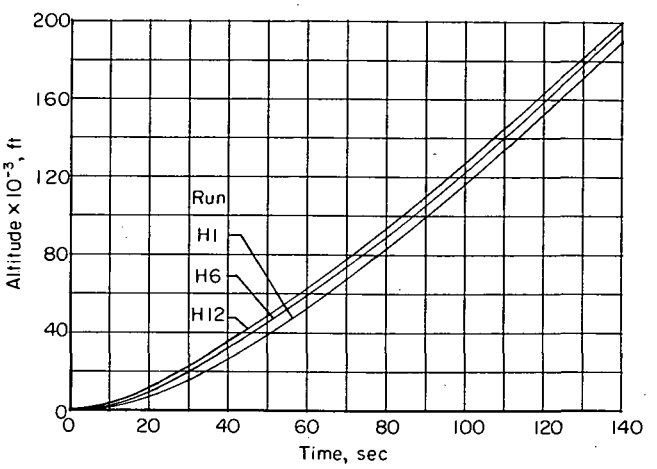

(a) Altitude.

Figure 11.- Time histories of representative cases during atmospheric flight. HTO.

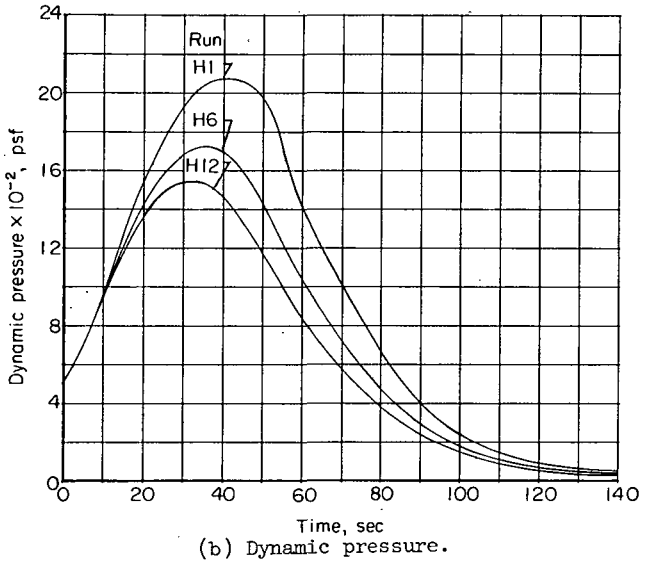

(b) Dynamic pressure.

Figure 11.- Continued.

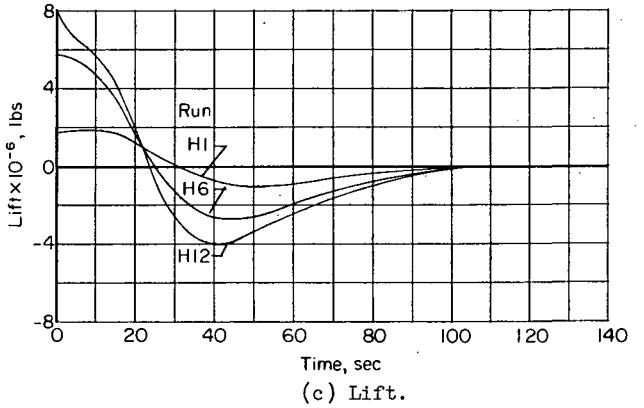

(c) Lift.

Figure 11.- Continued.

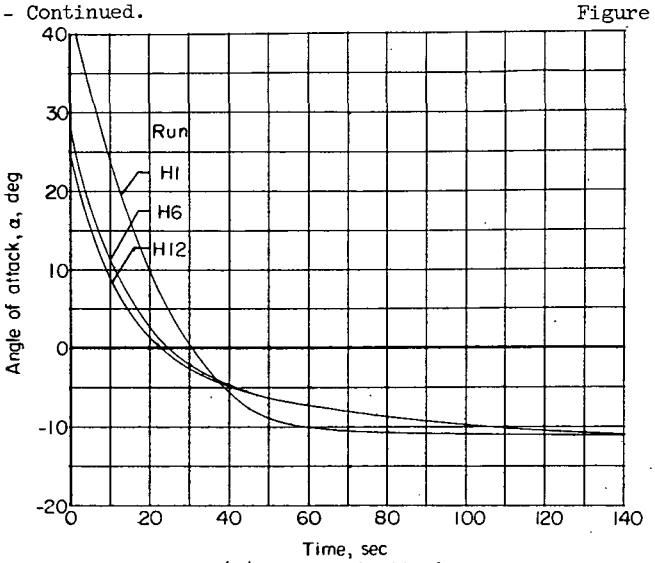

(d) Angle of attack.

Figure 11.- Concluded.

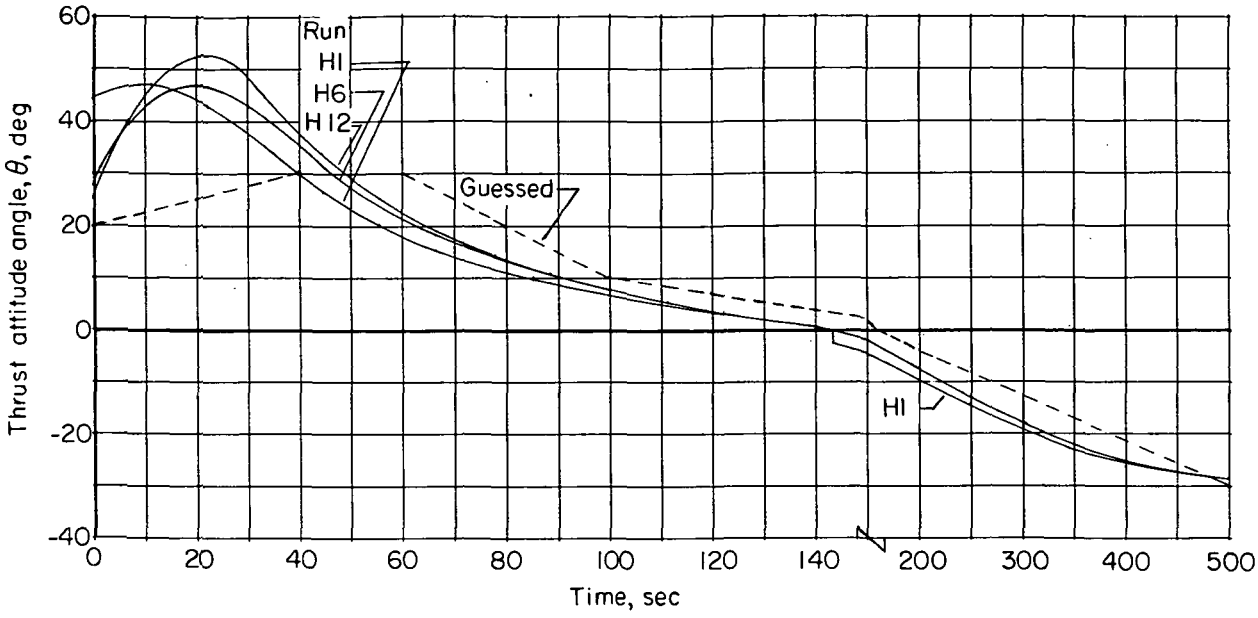

Figure 12.- Vehicle thrust attitude time history. HTO.

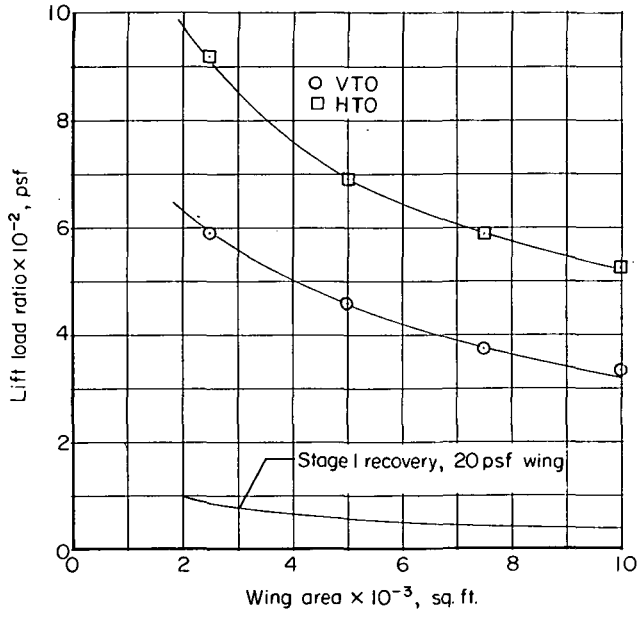

Figure 13.- Variation of the ratio of lift to total wing area with exposed wing area. VTO and HTO.

NASA-Langley, 1967